 doi:10.20944/preprints201807.0175.v1

Article

Computational Investigation on the Enantioselective Copper(I)-Catalyzed Addition of Enynes to Ketones

Hanwei Li [1], Mingliang Luo[1], Guohong Tao[1], and Song Qin [1]*

[1] Key Laboratory of Green Chemistry and Technology, Ministry of Education, College of Chemistry, Sichuan University, Chengdu, Sichuan, 610064, China;
* Correspondence: qinsong@scu.edu.cn; Tel.: +19-981-277-206

Abstract: Computational investigations on the BPE-ligated Cu-catalysed enantioselective addition of enynes to ketones were performed with DFT method. Two BPE-CuMes catalysts, BPE-CuMes and (*S,S*)-Ph-BPE–CuMes, were employed to probe the reaction mechanism with the emphasis on stereoselectivity. The calculations on the BPE-CuMes system indicate that the actvie metallized enyne intermediate acts as the catalyst for the catalytic cycle. The catalytic cycle involves two steps: 1) the ketone addition to the alkene moiety of the metallized enyne; 2) the metallization of enyne followed by the release of product with the recovery of the active metallized enyne intermediate. The first step accounts for the distribution of the products, and therefore is the stereo-controlling step in chiral systems. In the chiral (*S,S*)-Ph-BPE–CuMes system, the steric hindrance is vital for the distribution of products and responsible for the stereoselectivity of this reaction. The steric hindrance between the phenyl ring of the two substrates and groups at the chiral centers in the ligand skeleton is identified as the original of the stereoselectivity for the titled reaction.

Keywords: Copper-catalysed; Enantioselective; DFT

1. Introduction

Catalytic asymmetric nucleophilic addition of hydrocarbons to ketones is of great interest in organic synthesis, because this reaction is an effective method to obtain quaternary carbon centres [1-8]. Efavirenz and Tripanavir, two enzyme inhibitors with one or more tetrasubstituted centres in their structures are often used in the treatment of AIDS, and therefore such reactions are significant in many pharmaceutical drugs synthesis [1].

The pioneering work reported by Dosa and Fu in 1998 demonstrated that an excess of methanol allowed the addition of diphenyl zinc to aromatic and aliphatic ketones with fair to excellent enantioselectivities (up to 91% ee) [9]. In 2006, the asymmetric rhodium-catalyzed dienylation of α-ketoesters was reported by Krische group [10]. Then, the conjugated enynes were used as pronucleophiles for the introduction of the dienyl group in the presence of a Walphos rhodium(I) catalyst for the hydrogen mediate coupling on ketones [1]. Later, this catalytic method was applied to enantioselective reductive coupling of 1,3-enynes to heterocyclic aromatic aldehydes and ketones via rhodium-catalysed asymmetric reaction [11]. The use of substoichiometric amounts of chiral ligands for the asymmetric enantioselective alkynylation of ketones catalyzed by Zn (salen) complexes was pioneered in 2003 by Cozzi. Good reactivity was reached with a 20 mol% amount of the salen ligand with enantioselectivities up to 81% [12-16]. In 2004, Bolm and co-workers reported C_1-symmetric sulfoximines as ligands in copper-catalysted asymmetric Mukaiyama-type aldol reactions [17]. Aldol products have been obtained with up to 99% ee in high yield. Then, they developed a new ligand class consisting of C_1-symmetric aryl-bridged aminosulfoximines in this

Preprints (www.preprints.org) | NOT PEER-REVIEWED | Posted: 10 July 2018 doi:10.20944/preprints201807.0175.v1

reaction. Under the optimized reaction conditions, 10 mol% mixture of $Cu(OTf)_2$ and aminosulfoximine in THF have outstanding enantioselectivities (up to 99% ee) with yields up to 90% [18]. Shibasaki et al. developed a new methodology for the catalytic aldol reaction to ketones. This research group designed new chiral C_2-symmetric bidentate phosphine ligands. The success of this reaction depended on a unique, dynamic ligand exchange between silicon and copper atoms, and this method was applied to a catalytic enantioselective reaction [19].

Among the series of organometallic catalysis reactions, copper catalysis has offered an inexpensive, environmentally friendly alternative to the use of precious metals [20-29]. Shibasaki et al. described a possible solution to a catalytic enantioselective allylation of ketoimines. They developed the general basic methodology for allylation of ketoimines, this method used CuIF catalyst combined with $La(OiPr)_3$ cocatalyst and allylboronate as nucleophile [30]. Thus, the copper-based chiral catalysts for the asymmetric allylation of ketones attracts much attention. Kanai and Shibasaki successfully developed the Cu-DIFLUORPHOS complex-catalysed enantioselective alkylative aldol reactions and this reaction can be applied to a wide range of substrates. Allenic esters coupling with ketones and dialkyl zincs that deliver δ-lactones with excellent enantioselectivity (typically >95: 5 er.) [31,32]. Hoveyda and co-workers described the Cu-catalysed chemoselective and enantioselective addition to aldehydes and ketones with aryl or alkyl substituted allenes and $B_2(pin)_2$ (typically>95: 5 er.) [33]. Shimizu, Kanai and co-workers developed an efficient catalytic method to generate reactive allylcopper species (typically >95: 5 er). And the allylcopper can be used for subsequent asymmetric carbonyl allylation, providing 1H-isochromene derivatives in excellent enantioselectivity [34]. Hoveyda and co-workers demonstrated that the Proto-boryl additions to 1,1-disubstituted allenes in the presence of chiral NHC-Cu complexes, $B_2(pin)_2$, and *t*-BuOH proceed to afford vinyl boronates up to 98% yield, and in excellent yield (typically>95:5 er) [35]. Very recently, Motomu Kanai et al. reported a copper-catalyzed asymmetric addition of enynes to ketones with good functional group tolerance and this reaction does not require stoichiometric amounts of bases and additives. They also found that the species resulting from the coordination of (*S*,*S*)-Ph-BPE ligands to mesitylcopper (CuMes) is more reactive and efficient. In their work, (*S*,*S*)-Ph-BPE ligand has been introduced into the catalytic asymmetric nucleophilic addition of hydrocarbons to ketones at low temperature (–30°C) with high ee values [36].

Although there are so many experiments successful in the synthesis of target products, the above reactions mediated by the organometallic catalysts just give moderate ee values in general, which hinders the above asymmetric reactions to construct tetrasubstituted centres in practice. The detailed mechanism of such a copper-catalyzed asymmetric nucleophilic addition of enynes to ketones as well as the origin of the stereochemistry, however, is much less known. Although it is well known that the chiral environment is controlled by classical steric and electronic factors and the rigidity of the ligand framework, [36-49] the effects of chiral ligands on such asymmetric reactions are still uncertain. Therefore, it is hard to precisely evaluate the key parameters of chiral ligands associated with high ee values, which becomes an obstacle for designing new effective chiral ligands.

The present investigation focuses on the origin of the stereochemistry of asymmetric nucleophilic addition of enynes to ketones. In an attempt to gain a better understanding of the inner reasons of the asymmetric nucleophilic addition reaction at a molecular level and to clarify how the chiral BPE-ligated copper-catalysts enhance the reaction enantioselectivity, we here carry out theoretical simulations on such reaction systems based on quantum chemistry, and this work is expected to be useful for the design of new ligands.

2. Results and discussion

2.1 Mechanism of the BPE–CuMes model system

In this section, BPE–CuMes is used as the model species to probe the reaction mechanism. As shown in Scheme 1, the calculations predict that the entire reaction could be roughly divided to the following two prats: 1) the exchange of hydrogen from the α-H of alkyne moiety in enyne to Mes

Preprints (www.preprints.org) | NOT PEER-REVIEWED | Posted: 10 July 2018 doi:10.20944/preprints201807.0175.v1

fragment at copper centre with the formation of active intermediate IM2 and 2) the catalytic cycle to generate the final product with the recovery of the intermediate IM2.

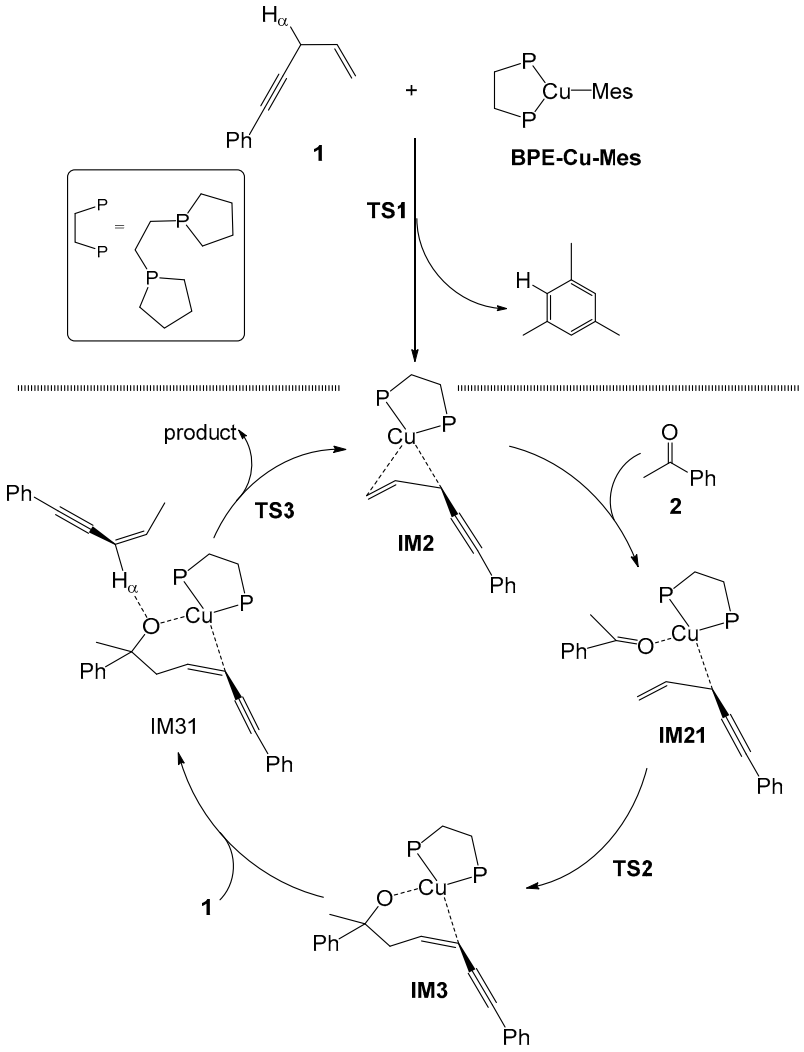

Scheme 1. Schematic diagram of the reaction process in the BPE-ligated system

2.1.1 Formation of the active intermediate IM2

The optimized structures at the M06/6-31G(d,p) level and the relative energies diagram at the M06(SMD, THF)/6-311+G(d,p) level in the modelled PBE-ligated system are depicted in Fig 1 and 2, respectively.

First, the reaction is trigged by the coordination of the modelled ligand BPE to the copper-end in MesCu, which generates BPE-CuMes complex. This complex is featured by a tridentate-coordinated copper centre with two Cu-P bonds of 2.232 and 2.205 Å, respectively, and the P-Cu-P bite angle is calculated to be 89.3°. SMD calculations give that this coordination step is benefited by 126.0 kJ mol^{-1} in the Gibbs free energies in THF, suggesting that this species is easy to be generated.

Preprints (www.preprints.org) | NOT PEER-REVIEWED | Posted: 10 July 2018 doi:10.20944/preprints201807.0175.v1

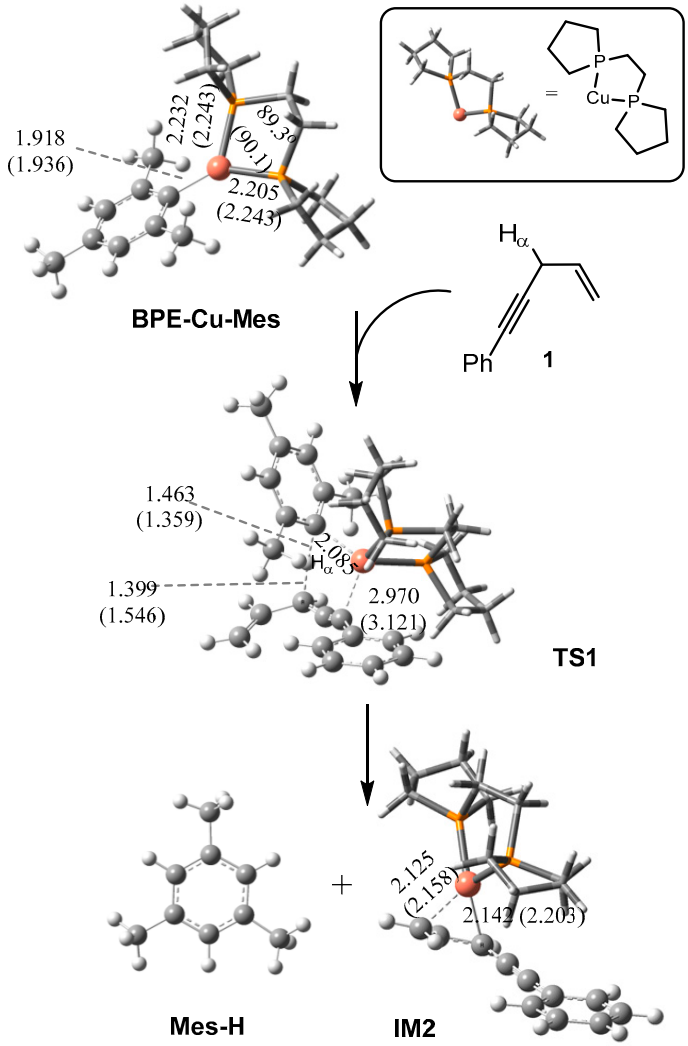

Figure 1. Optimized structures along the reaction form the reactants to IM2 at the M06/6-31G(d,p) level and B3LYP/6-31G(d,p) in parentheses. Bond lengths are in angstroms and the angle are in degrees.

Next, an external substrate 1-phenyl-4-penten-1-yne **1** gets close to the BPE-Mes-Cu complex accomplished by cleavage of the C–H(α) bond of alkyne moiety via **TS1**. This species is characterized by an elongated C–H(α) bond of 1.399 Å and a shortened C(Mes)–H bond of 1.463 Å. This step corresponds to the migration of one α-hydrogen from substrate 1 to the Mes moiety. As a result, the exchange of hydrogen from enyne moiety to Mes fragment takes place, which is followed by the release of one mesitylene (MesH) molecule and the formation of intermediate **IM2**. SMD calculations indicate the above step benefits 68.7 kJ mol^{-1} in Gibbs free energies with a moderate energy barrier of 112.3 kJ mol^{-1}, meaning that the formation of **IM2** is favoured in thermodynamics.

For **IM2**, the Cu-C(α) distance of 2.142 Å with the occupied orbital of 1.996e from NBO analysis identify **IM2** as a metallized enyne species.

Preprints (www.preprints.org) | NOT PEER-REVIEWED | Posted: 10 July 2018 doi:10.20944/preprints201807.0175.v1

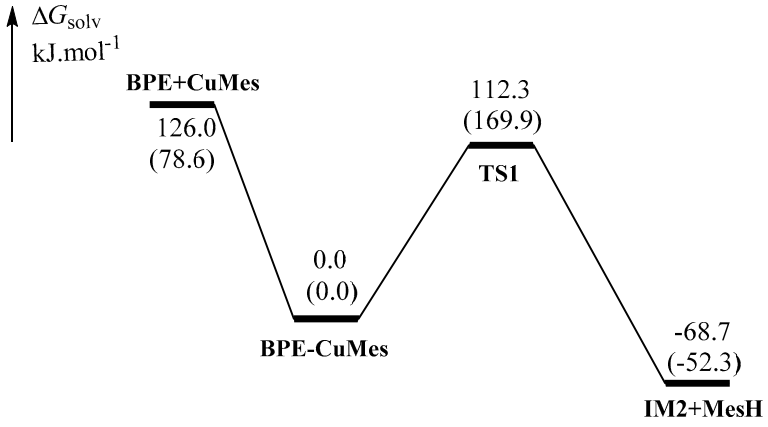

Figure 2. Energy diagram for the formation of the intermediate IM2. ΔG_{solv} (in kJ mol^{-1}) are calculated at the M06(SMD,THF)/6-311+G(d,p) level; ΔG_{solv} (in kJ mol^{-1}) at the B3LYP/(SMD,THF)/6-311+G(d,p) level are listed in parentheses .

3.1.2 Catalytic cycle over **IM2**

The optimized structures at the M06/6-31G(d,p) level and the SMD energies diagram at the M06/6-311+G(d,p) level along the catalytic cycle in the modelled BPE-ligated system are depicted in Figure 3 and 4, respectively.

As shown in Figure 3, the catalytic cycle starts from the coordination of an acetophenone **2** molecule getting close to the copper-end of **IM2** accomplished by the attack of carbonyl to the ene-end of metallized enyne via **TS2**.

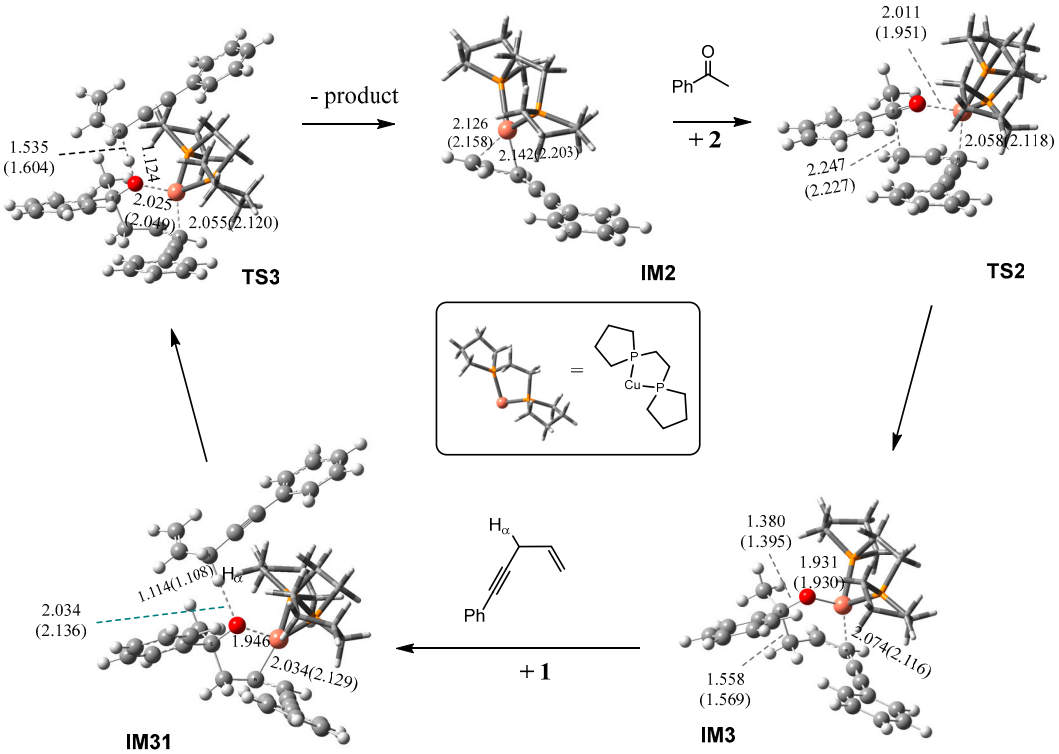

Figure 3. Optimized structures along the catalytic cycle at the M06/6-31G(d,p) level and B3LYP/6-31G(d,p) in parentheses. Bond lengths are in angstroms and the angle are degrees.

Preprints (www.preprints.org) | NOT PEER-REVIEWED | Posted: 10 July 2018 doi:10.20944/preprints201807.0175.v1

For **TS2**, the closet C–C distance between carbonyl and ene moieties shortens to 2.247Å. This suggests that the formation of the C–C bond occurs with the ketone addition to the double bond of 1-phenyl-4-penten-1-yne. In IM3, the C(carbonyl)–C(eneye) bond of 1.558Å indicate that acetophenone addition to the 1-phenyl-enyne completed. SMD calculations indicate the above step benefits 47.4 kJ mol^{-1} in Gibbs free energies with a smaller energy barrier of 60.0 kJ mol^{-1}, meaning that this ketone addition process is easy to occur.

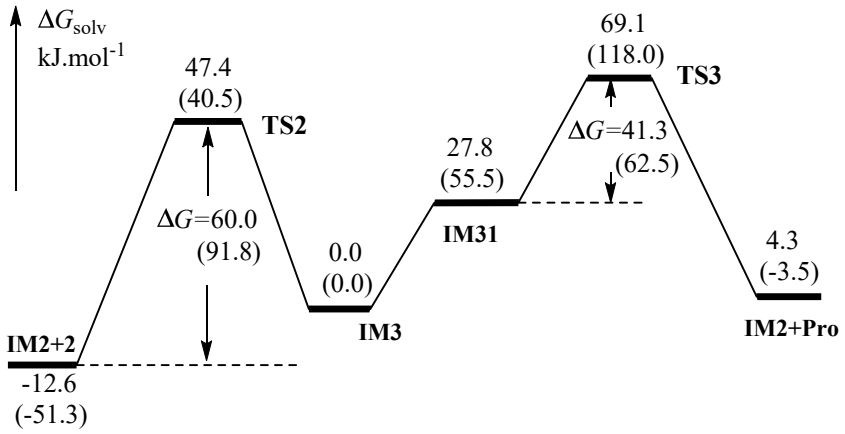

Figure 4. Evolution of energies along the reaction routes in the THF system. ΔG_{solv} (in kJ mol^{-1}) for various species are calculated at the M06(SMD, THF)/6-311+G(d,p) level; ΔG_{solv} (in kJ mol^{-1}) at the B3LYP(SMD, THF)/6-311+G(d,p) level are listed in parentheses .

From **IM3**, another **1** could interacts with the O-end of **IM3** with the formation of molecule-molecule complex **IM31**. For **IM31**, the linear C–H(α)···O pattern with the C–H(α) and the O–H(α) bond of 1.114 and 2.034 Å show that there might be a hydrogen bond to connect **IM3** and the external **1**.

From **IM31**, the reaction continues to generate the final product with the recovery of active intermediate **IM2** via **TS3**. In **TS3**, the O–H(α) bond is remarkably decreased to 1.124 Å, and C–H(α) bond increases to 1.535 Å. This suggests that he O–H(α) bond forms with the cleavage of the C–H(α) bond of the external 1, which corresponds to the metallization of substrate enyne in the catalytic cycle. SMD calculations indicate the above step with a smaller energy barrier of 41.3 kJ mol^{-1} in Gibbs free energies.

Combined with the reaction mechanism in part **1** and **2** in the model BPE-ligated system, it could be found that the formation of the active intermediate **IM2** is vital for the catalytic reaction. In part **1**, **IM2** is generated from the metallization of enyne via **TS1** with the energy barrier of 112.3 kJ mol^{-1}. However, once **IM2** results, the metallization of enyne could advantageously take place via TS3, for this step bearing a relatively smaller energy barrier of 41.3 kJ mol^{-1}. Therefore, the active intermediate **IM2** plays the role as the real catalyst for the reaction and BPE-Cu-Mes acts as a precursor.

As shown in Figure 4, to obtain the final products, the reaction must overcome two energy summits located at **TS2** and **TS3** in catalytic cycle. SMD calculations (both M06 and B3LYP) predict the larger barrier via **TS2** in catalytic cycle, which means that the metallization of enyne via **TS2** should be the rate-determining step (RDS) for this reaction.

Preprints (www.preprints.org) | NOT PEER-REVIEWED | Posted: 10 July 2018 doi:10.20944/preprints201807.0175.v1

On the other hand, SMD calculations place **TS2** on the energy top in the catalytic cycle. It should be emphasized that the distribution of products should be predominantly depend on the evolution of **IM3** in the energy trap. Because the reverse energy barrier from **IM3** to **IM2** via **TS2** is much larger than **IM31** to product via **TS3**, if **IM3** forms, the reverse process to reactants is hindered and the reaction should give rise to the final products irreversibly. Therefore, it is reasonable to deduce that **TS2**, corresponding to ketone addition step, is the stereo-controlling transition state under the asymmetric factors introduced in the reaction systems.

3.2 Stereochemistry of such reactions

In order to explore the factors controlling stereoselectivity in detail, we extend our calculations on the chiral ligated reaction system based on the (*S*,*S*)-Ph-BPE diphosphate ligands (see Computational Details). This ligand has been found to possess remarkable chiral recognition ability and broad applicability in various transitional metal-catalysed asymmetric reactions, and was successfully employed in the asymmetric titled reactions. In the series of reports on asymmetric reaction of ketones, the yields of such reactions are respectable with excellent enantioselectivities as high as 97% (*R*-product) [36].

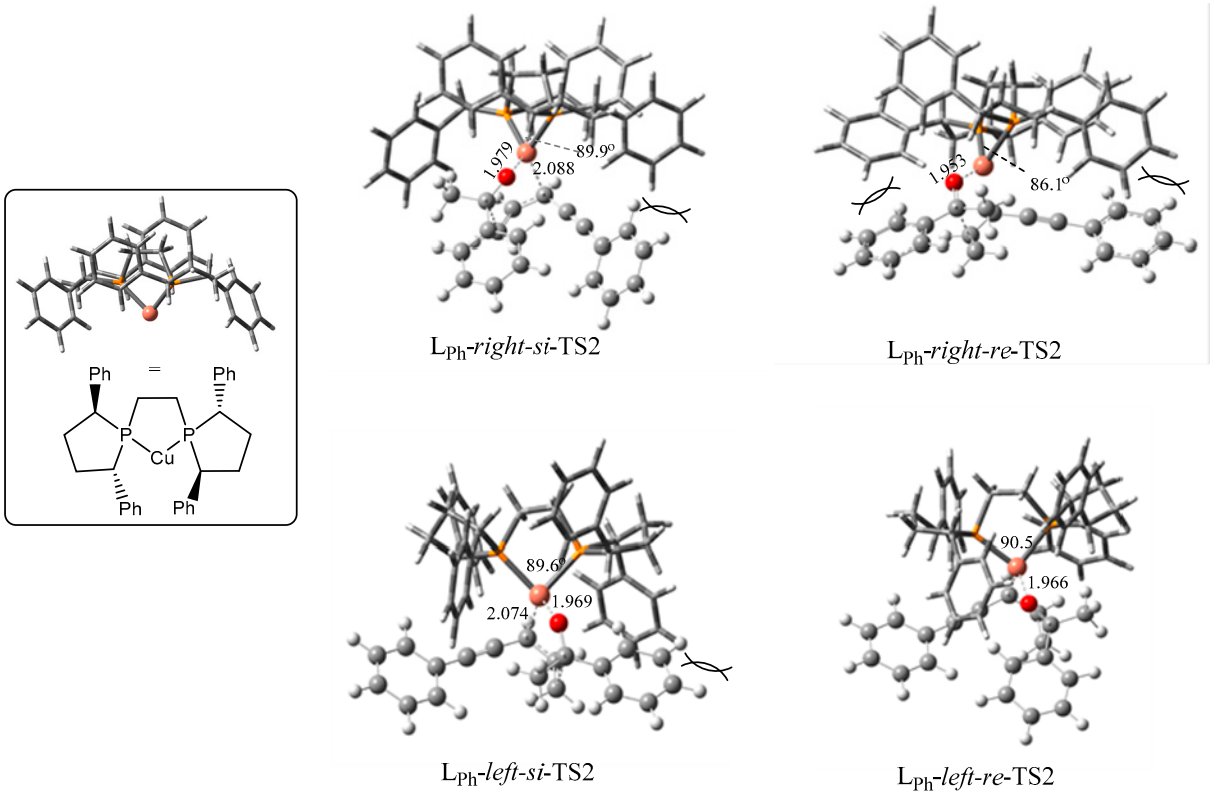

Figure 5. 3D model of stereo-controlling transition states (**TS2**s) at the M06/6-31G(d,p) lvel in the(*S*,*S*)-Ph-BPE ligand system.

As mentioned above, the distribution of the racemic products is closely controlled in the ketone addition step. Therefore, to reduce computational costs, the following investigations on the stereochemistry of these ligated systems just focus on the structures of addition transition states (**TS2**s). The optimized **TS2**s are provided in Figure 5[to give brief expression, (*S*,*S*)-Ph-BPE is marked

Preprints (www.preprints.org) | NOT PEER-REVIEWED | Posted: 10 July 2018 doi:10.20944/preprints201807.0175.v1

as LPh]. The configuration of products and the SMD energies of these **TS2**s at the M06/6-311+G(d,p) level are summarized in Table 1.

3.2.1 Stereoselectivity of (S, S)-Ph-BPE system

Similar to model system, these four ligated-Cu catalysts also bear a gross structure of P–Cu–P network. These **TS2**s are characterized by the location of the phenyl ring of enyne with respect to the ligand. For these ligands possess C_2-symmetry, in the structure of the right-**TS2**s, the phenyl ring of enyne keeps almost on the right side in Figure 5. In contrast, the phenyl ring of enyne could alternatively adopt on the left side for the left-**TS2**s. Besides, two attack modes of enyne to the ketone are available: in re-**TS2**s, the enyne could attack ketone from re-face to raise the product in *R*-configuration; while in si-**TS2**s, the enyne could attack ketone from si-face to generate the product in *S*-configuration. Therefore, in the actual system, four transition states results: L_{Ph}-right-re-**TS2** and L_{Ph}-left-re-**TS2** could provide the final product in *R*-configuration; the other two L_{Ph}-right-si-**TS2** and L_{Ph}-left-si-**TS2** generate the final product in *S*-configuration.

Table 1. ΔG values of competing TS2s in (*S*,*S*)-Ph-PBE system.

TS2s	P-Cu-P angle	Configuration of products	ΔG (kJ/mol)
L_{Ph}-right-si	89.9°	S	15.6
L_{Ph}-right-re	86.1°	R	43.5
L_{Ph}-left-si	89.6°	S	33.4
L_{Ph}-left-re	90.5°	R	0.0

For the (*S*,*S*)-Ph-BPE-ligated system, it is could be distinguished that two kinds of hindrance available: mode a) the hindrance between the phenyl ring of ligand and phenyl of enyne; mode b) the hindrance between the phenyl ring of ligand and phenyl of acetophonone. The LPh-right-si-TS2 suffers the hindrance in mode a; the L_{Ph}-left-si-**TS2** bears the hindrance in mode b, respectively. Also, there exists the hindrance in two modes for the L_{Ph}-right-re-**TS2**, and there exists no remarkable hindrance for the the L_{Ph}-left-re-**TS2**. The calculations place L_{Ph}-left-re-**TS2** 15.6 kJ mol^{-1} at the M06(SMD)/6-311+G(d,p) level and 16.3 kJ mol^{-1} at the B3LYP(SMD)/6-311+G(d,p) level lower than the competing translon state L_{Ph}-right-si-**TS2** in Gibbs free energies. Because *R*-configuration product is yielded from L_{Ph}-left-re-**TS2**, *R*-product would be the predominant product with high ee value in the titled addition reaction, which is in good agreement with the experimental observation (*R*-product with 97% ee) [36].

Furthermore, it is worth mentioned that for the above four transition states, the energy discrepancy is related to the P–Cu–P bite angle. The larger P–Cu–P angle means the lighter tension of (*S*,*S*)-Ph-BPE-Cu moiety which is associated with the smaller hindrance suffered in L_{Ph}-**TS2**s, and therefore makes this transition state favoured in relative energies.

Preprints (www.preprints.org) | NOT PEER-REVIEWED | Posted: 10 July 2018 doi:10.20944/preprints201807.0175.v1

Table 2. ΔG values of competing TS2s in (S,S)-Me-PBE system calculated at the different levels

TS2s	$\Delta G_{solv\text{-}M06}$	$\Delta G_{solv\text{-}B3}$	$\Delta G_{gas\text{-}M06}$	$\Delta G_{gas\text{-}B3}$
L_{Ph}-right-si	15.6	16.3	6.2	12.0
L_{Ph}-right-re	43.5	30.8	26.9	25.4
L_{Ph}-left-si	33.4	23.2	19.4	21.1
L_{Ph}-left-re	0.0	0.0	0.0	0.0

$\Delta G_{solv\text{-}M06}$ (in kJ mol^{-1}) are calculated at the M06(SMD,THF)/6-311+G(d,p) level in THF solvent; $\Delta G_{solv\text{-}B3}$ (in kJ mol^{-1}) are calculated at the B3LYP(SMD,THF)/6-311+G(d,p) level in THF solvent; $\Delta G_{gas\text{-}M06}$ (in kJ mol^{-1}) are calculated at the M06/6-31G(d,p) level in the gas-phase; $\Delta G_{gas\text{-}B3}$(in kJ mol^{-1}) are calculated at the B3LYP/6-31G(d,p) level in the gas-phase.

3.2.2 Origin of stereoselectivity

Next, the aim of the present investigation turns to the origin of the stereochemistry of the titled reaction and the influencing factor of groups at chiral sites of BPE ligand on it. Here, we used methyl group smaller in size to take place the phenyl rings at (*S*,*S*)-BPE skeleton. The four-transition state L_{Me}-**TS2**s and the relative energies are shown in Figure 6.

As shown in Figure 6, no remarkable hindrance between ligand and substrates could be found out, which might be confirmed by the larger P–Cu–P angles (>90°). Correspondingly, the calculations place the energy gap between two competing transition states ca. 0.2 kJ mol-1 thus no obvious enantioselectivity could be detected.

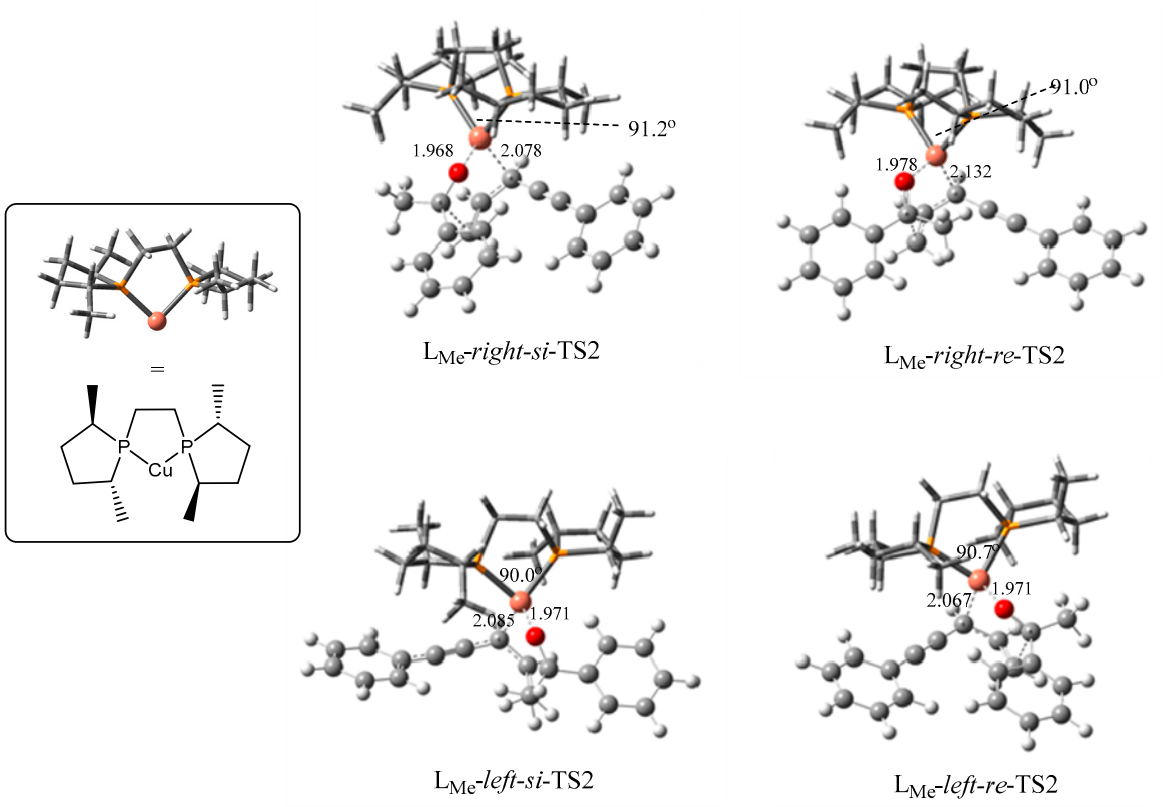

Figure 6. 3D model of stereo-controlling transition states (**TS2**s) at the M06/6-31G(d,p) in the(*S*,*S*)-Me-BPE ligand system.

Preprints (www.preprints.org) | NOT PEER-REVIEWED | Posted: 10 July 2018 doi:10.20944/preprints201807.0175.v1

To sum up, the enantioselectivity should be controlled by the steric hindrance between of substrates and ligands. When larger size groups exist at the chiral sites of the catalyst, they could selectively make one of the competing transition states stable in terms of control the orientation of two substrates with respect to the C_2-symmtry ligand. In the (*S*,*S*)-Ph-BPE system, *R*-configuration catalyst makes left-re-**TS2** stable with the larger P–Cu–P, and therefore leads to the predominant *R*-product. Moreover, it is also found that ee value is significantly depended on the size of the groups at the chiral sites of ligand: when larger groups are introduced at the chiral sites of BPE, ΔG between two competing transition states becomes greater enough for high ee value.

Table 3. ΔG values of competing **TS2**s in (S,S)-Me-PBE system.

TS2s	P-Cu-P angle	Configuration of products	ΔG_{solv} (kJ/mol)
L_{Me}-right-si	91.2°	S	0.0
L_{Me}-right-re	91.0°	R	13.3
L_{Me}-left-si	90.0°	S	17.3
L_{Me}-left-re	90.7°	R	0.7

4. Models and Computational Methods

The previous computational literature demonstrated that the M06 [50-53] and B3LYP methods performed well for catalytic reactions based on the copper system [54-61]. In the present investigation, the geometrical optimizations of all the intermediates (**IM**) and transition states (**TS**) were performed using the M06 and B3LYP method with the 6-31G(d,p)[62] basis set for all atoms. To take the entropy effects in solvents into account, single-point self-consistent reaction field (SCRF) calculations based on the SMD [63-71] model with radii=UAHF keyword were carried out on the gas-phase optimized geometries for all species. As THF was used as the solvent in the actual experiments [72], the latter calculations in actual system were carried out with a dielectric constant ε= 7.43 for the solvent THF. For evaluating the solvent effects, the free energies were calculated at the M06/6-311+G(d,p)[55,73] level and added to the gas-phase free energy to obtain the Gibbs energy in THF (G_{solv}) at 298.15 K. Unless otherwise stated, G_{solv} is used in the discussion and the energy levels refer to the G_{solv} scale.

All calculations were performed with the Gaussian 09 program [74]. Frequencies were calculated at the same level to confirm each stationary point to be either a minimum (no imaginary frequency) or a saddle point (unique imaginary frequency), and to obtain the zero-point correction. Details of the preliminary results are listed in the ESI. †

The major work in the present investigation is based on the following two models. (see Scheme 2.)

Preprints (www.preprints.org) | NOT PEER-REVIEWED | Posted: 10 July 2018 doi:10.20944/preprints201807.0175.v1

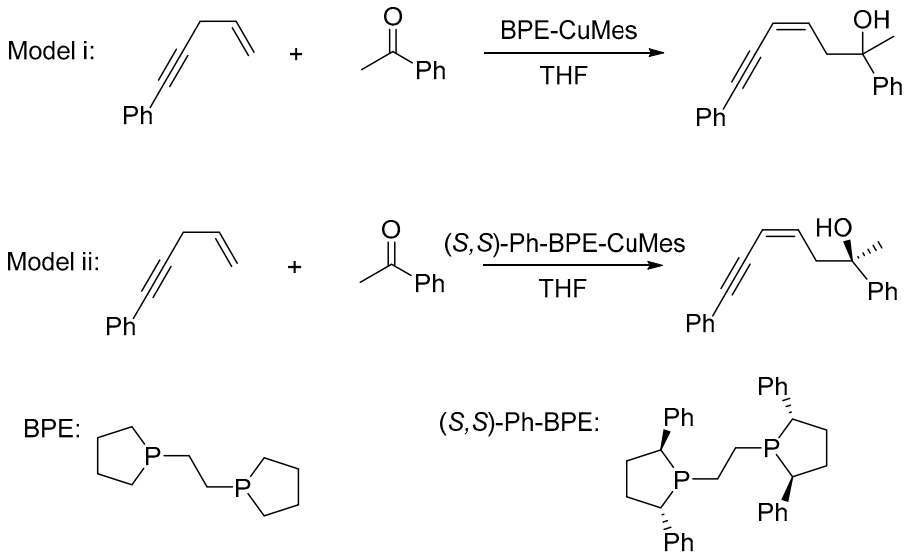

Scheme 2. Used models in the present calculation.

Model i: BPE-Cu-Mes system

The CuMes-catalysed asymmetric reduction of carbonyl compounds, suggested that the metal source with a 1: 1 ratio of ligand to metal is involved. Therefore, the BPE-CuMes species in monomeric form was constructed in the present calculations.

In this section, 1-phenyl-4-penten-1-yne **1** and acetophenone **2** was employed as the substrates. The modelled non-chiral phosphine ligand BPE was introduced in the present investigation, and a monomeric ligated CuMes species was constructed as the catalytic species (Scheme 1). This treatment is designed to probe the reaction mechanism at less computational cost with acceptable calculated precision.

Model ii: Chiral-(S,S)-Ph-BPE-Cu-Mes model

In this section, a chiral diphosphine ligand (S,S)-Ph-BPE-CuMes was introduced into the reaction system. This system has been used in experiments and proven to be excellent in catalytic asymmetric nucleophilic addition of conjugated acetophenone with high ee (97%) values [36].

5. Conclusions

The results from the present investigations on the BPE-ligated Cu-catalysed enantioselective addition of enynes to ketones were summarized as follows:

For the modelled BPE-Cu-Mes system, the calculations on the BPE-MesCu system, predicts that the active metallized enyne intermediate acts as the catalyst for the catalytic cycle. The catalytic cycle involves two steps: 1) the ketone addition to the alkene moiety of the metallized enyne; 2) the metallization of enyne followed by the release of product with the recovery of the active metallized enyne intermediate. The first step accounts for the distribution of the products, and therefore is the stereo-controlling step in chiral system.

In the chiral (S,S)-Ph-BPE–MesCu system, the calculation identify that the steric hindrance between the phenyl ring of the two substrates and groups at the chiral centres in the ligand skeleton to be the origin of the stereoselectivity for the titled reaction. The stereoselectivity of this reaction is sensitive to the size of the groups at the chiral centres of BPE ligand.

Supplementary Materials: The following are available online.

Author Contributions: H. L. performed the experiments and wrote the paper; S. Q. conceived, designed, and performed the experiments and discussed the results. M. L. and G. T. supported the analysis of data.

Funding: This research was funded by [National Natural Science Foundation of China] grant number [21303108].

Acknowledgments: The finance support from the National Natural Science Foundation of China (No. 21303108) is gratefully acknowledged.

Conflicts of Interest: The authors declare no conflict of interest.

References

1. Riant, O.; Hannedouche, J. Asymmetric catalysis for the construction of quaternary carbon centres: nucleophilic addition on ketones and ketimines, *Org. Biomol. Chem.* **2007**, *5*, 873-888.
2. Corey, E. J.; Guzman-Perez, A. The Catalytic Enantioselective Construction of Molecules with Quaternary Carbon Stereocenters，*Angew. Chem. Int. Ed*. **1998**, *37*, 388-401.
3. Fuji, K.; Asymmetric Creation of Quaternary Carbon Centers，*Chem. Rev.* **1993**, 93, 2037-2066.
4. Douglas, C. J.; Overman, L. E.; Catalytic asymmetric synthesis of all-carbon quaternary stereocenters，*Proc. Natl. Acad. Sci. U. S. A.* **2004**, *101*, 5363-5367.
5. Abozeid, M. A.; Sairenji, S.; Takizawa, S.; Fujita, M.; Sasai, H. Enantioselective synthesis of tetrahydrocyclopenta[b]-indole bearing a chiral quaternary carbon center via Pd(II)–SPRIX-catalyzed C–H activation，*Chem. Commun.* **2017**, *53*, 6887-6890.
6. Ghorai, M. K.; Halder, S.; Das, S.; Domino Michael-Michael and Aldol-Aldol Reactions: Diastereoselective Synthesis of Functionalized Cyclohexanone Derivatives Containing Quaternary Carbon Center. *J. Org. Chem.* **2015**, *80*, 9700-9712.
7. Yi, Y.; Lee, H.; Ho Jun, C. Rh(III)-catalyzed C–H activation reactions forming 1H-isoindoles containing a quaternary carbon center from aryl ketones or benzylamines，Chem.Commun. **2016**, *52*, 10171-10174.
8. Franckevičius, V. Palladium-catalyzed construction of quaternary carbon centers with propargylic electrophiles，*Tetrahedron Letters*. **2016**, *57*, 3586-3595.
9. Dosa, P. I.; Fu, G. C. Catalytic Asymmetric Addition of ZnPh2 to Ketones: Enantioselective Formation of Quaternary Stereocenters. *J. Am. Chem. Soc.* **1998**, 120, 445-446.
10. Kong, J. R.; Ngai, M. Y.; Krische, M. J. Highly Enantioselective Direct Reductive Coupling of Conjugated Alkynes and α-Ketoesters via Rhodium-Catalyzed Asymmetric Hydrogenation. *J. Am. Chem. Soc.* **2006**, *128*, 718-719.
11. Komanduri, V.; Krische, M. J. Enantioselective Reductive Coupling of 1,3-Enynes to Heterocyclic Aromatic Aldehydes and Ketones via Rhodium-Catalyzed Asymmetric Hydrogenation: Mechanistic Insight into the Role of Brønsted Acid Additives. *J. Am. Chem. Soc.* **2006**, *128*, 16448-16449.
12. Cozzi, P. G. Enantioselective Alkynylation of Ketones Catalyzed by Zn(Salen) Complexes. *Angew. Chem., Int. Ed.* **2003**, *42*, 2895-2898.
13. Jiang, B.; Chen, Z.; Tang, X. Highly Enantioselective Alkynylation of α-Keto Ester: An Efficient Method for Constructing a Chiral Tertiary Carbon Center. *Org. Lett*. **2002**, *4*, 3451-3453.
14. Pu, L. Asymmetric alkynylzinc additions to aldehydes and ketones. *Tetrahedron*. **2003**, *59*, 9873-9886.
15. Cozzi, P. G.; Hilgraf, R.; Zimmermann, N. Acetylenes in Catalysis: Enantioselective Additions to Carbonyl Groups and Imines and Applications Beyond. *Eur. J. Org. Chem*. **2004**, 4095-4105.
16. Lu, G.; Li, Y. -M.; Li, X. -S.; Chan, A. S. C. Synthesis and application of new chiral catalysts for asymmetric alkynylation reactions. *Chem. Rev*. **2005**, *249*, 1736-1744.
17. Langner, M.; Bolm, C.; C_1-Symmetric Sulfoximines as Ligands in Copper-Catalyzed Asymmetric Mukaiyama-Type Aldol Reactions. *Angew. Chem., Int. Ed*. **2004**, *43*, 5984-5987.
18. Langner, M.; Rémy, P.; Bolm, C. Highly Modular Synthesis of C_1-Symmetric Aminosulfoximines and Their Use as Ligands in Copper-Catalyzed Asymmetric Mukaiyama-Aldol Reactions. *Chem. Eur. J.* **2005**, *11*, 6254-6255.
19. Oisaki, K.; Suto,Y.; Kanai, M.; Shibasaki, M. A New Method for the Catalytic Aldol Reaction to Ketones. *J. Am. Chem. Soc*. **2003**, *125*, 5644-5645.
20. Müller, D. S.; Marek, I.; Copper mediated carbometalation reactions. *Chem. Soc. Rev*. **2016**, *45*, 4552-4556.

21. Zhu, X.; Chiba, S. Copper-catalyzed oxidative carbon–heteroatom bond formation: a recent update. *Chem. Soc. Rev*. **2016**, *45*, 4504-4523.
22. Shibasaki, M.; Kanai, M. Asymmetric Synthesis of Tertiary Alcohols and α-Tertiary Amines via Cu-Catalyzed C-C Bond Formation to Ketones and Ketimines. *Chem. Rev*. **2008**, *108*, 2853-2873.
23. Thapa, S.; Shrestha, B.; Gurung, S. K.; Giri, R. Copper-catalysed cross-coupling: an untapped potential. *Org. Biomol. Chem*. **2015**,*13*, 4816-4827.
24. Maaliki, C.; Thiery, E. J. Thibonnet, Emergence of Copper-Mediated Formation of C–C Bonds. *Eur. J. Org. Chem.* **2017**, 209-228.
25. Yoshikai, N.; Nakamura, E. Mechanisms of Nucleophilic Organocopper(I) Reactions. *Chem. Rev*. **2012**, *112*, 2339-2372.
26. Jumde, R. P.; Lanza, F.; Veenstra, M. J.; Harutyunyan, S. R. Catalytic asymmetric addition of Grignard reagents to alkenyl-substituted aromatic N-heterocycles. *Science*, **2016**, 352, 433-437.
27. Yang, Y.; Perry, I. B.; Buchwald, S. L.; Copper-Catalyzed Enantioselective Addition of Styrene-Derived Nucleophiles to Imines Enabled by Ligand-Controlled Chemoselective Hydrocupration. *J. Am. Chem. Soc.* **2016**, *138*, 9787-9790.
28. Kubota, K.; Watanabe, Y.; Hayama, K.; Ito, H. Enantioselective Synthesis of Chiral Piperidines via the Stepwise Dearomatization/Borylation of Pyridines. *J. Am. Chem. Soc*. **2016**, *138*, 4338-4341.
29. Hojoh, K.; Ohmiya, H.; Sawamura, M. Synthesis of α-Quaternary Formimides and Aldehydes through Umpolung Asymmetric Copper Catalysis with Isocyanides. *J. Am. Chem. Soc*. **2017**, *139*, 2184-2187.
30. Wada, R.; Shibuguchi, T.; Makino, S.; Oisaki, K.; Kanai, M.; Shibasaki, M. Catalytic Enantioselective Allylation of Ketoimines. *J. Am. Chem. Soc*. **2006**, *128*, 7687-7691.
31. Oisaki, K.; Zhao, D.; Kanai, M.; Shibasaki, M. Catalytic Enantioselective Alkylative Aldol Reaction: Efficient Multicomponent Assembly of Dialkylzincs, Allenic Esters, and Ketones toward Highly Functionalized δ-Lactones with Tetrasubstituted Chiral Centers. *J. Am. Chem. Soc*. **2007**, *129*, 7439-7443.
32. Pulis, A. P.; Yeung, K.; Procter, D. J. Enantioselective copper catalysed, direct functionalisation of allenes via allyl copper intermediates. *Chem. Sci*. **2017**, *8*, 5240-5247.
33. Meng, F.; Jang, H.; Jung, B.; Hoveyda, A. H. Cu-catalyzed Chemoselective Preparation of 2-（Pinacolato）boron Substituted Allylcopper Complexes and their In Stitu Site-, Diastereo-, and Enantioselective Additions to Aldehydes and Ketones. *Angew. Chem., Int. Ed*. **2013**, *52*, 5046-5051.
34. Kawai, J.; Chikkade, P. K.; Shimizu, Y.; Kanai, M. In situ Catalytic Generation of Allylcopper Species for Asymmetric Allylation: Toward 1H-Isochromene Skeletons. *Angew. Chem., Int. Ed*. **2013**, *52*, 7177-7180.
35. Jang, H.; Jung, B.; Hoveyda, A. H. Catalytic Enantioselective Protoboration of Disubstituted Allenes. Access to Alkenylboron Compounds in High Enantiomeric Purity. *Org. Lett*. **2014**, *16*, 4658-4661.
36. Wei, X. F.; Xie, X. W.; Shimizu, Y; Kanai, M.; Copper(I)-Catalyzed Enantioselective Addition of Enynes to Ketones. *J. Am. Chem. Soc.* **2017**, *139*, 4647-4650.
37. Shimizu, H.; Nagasaki, I.; Saito, K.; Recent advances in biaryl-type bisphosphine ligands. *Tetrahedron.* **2005**, *61*, 5405-5432.
38. Lipshutz, B. H.; Keith, J.; Papa, P.; Vivian, R. A convenient, efficient method for conjugate reductions using catalytic quantities of Cu(I). *Tetrahedron Lett*. **1998**, *39*, 4627-4630.
39. Lipshutz, B. H.; Frieman, B. A.; Tomaso Jr, A. E.; Copper-in-Charcoal (Cu/C): Heterogeneous, Copper-Catalyzed Asymmetric Hydrosilylations. *Angew. Chem*. **2006**, *118*, 1281-1286.
40. Lipshutz, B. H.; Servesko, J. M. CuH-Catalyzed Asymmetric Conjugate Reductions of Acyclic Enones. *Angew. Chem*. **2003**, *115*, 4937-4940.
41. Lipshutz, B. H.; Frieman, B. A. CuH in a Bottle: A Convenient Reagent for Asymmetric Hydrosilylation, *Angew. Chem. Int. Ed.* **2005**, *44*, 6345-6348.
42. Lipshutz, B. H.; Papa, P. Copper-Catalyzed Reductive Alkylations of Enones: A Novel Transmetalation Protocol. *Angew. Chem*. **2002**, *114*, 4762-4764.
43. Lipshutz, B. H.; Servesko, J. M.; CuH-Catalyzed Asymmetric Conjugate Reductions of Acyclic Enones. *Angew. Chem. Int. Ed.* **2003**, *42*, 4789-4792.
44. Lipshutz, B. H.; Servesko, J. M.; Petersen, T. B.; Papa, P. P.; Lover, A. A.; Asymmetric 1,4-Reductions of Hindered â-Substituted Cycloalkenones Using Catalytic SEGPHOS−Ligated CuH. *Org. Lett*. **2004**, *6*, 1273-1275.
45. Lipshutz, B. H.; Tanaka, N.; Ta, B. R.; Lee, C. T. Chiral Silanes via Asymmetric Hydrosilylation with Catalytic CuH. *Org. Lett*. **2006**, *8*, 1963-1966.

46. Baker, B. A.; Bošković, Ž. V.; Lipshutz, B. H. (BDP)CuH: A "Hot" Stryker's Reagent for Use in Achiral Conjugate Reductions. *Org. Lett*. **2008**, *10*, 289-292.
47. Gallagher, B. D.; Taft, B. R.; Lipshutz, B. H. Asymmetric Conjugate Reductions of Coumarins. A New Route to Tolterodine and Related Coumarin Derivatives. *Org. Lett*. **2009**, 11, 5374-5377.
48. Lipshutz, B. H.; Servesko, J. M.; Taft, B. R. Asymmetric 1,4-Hydrosilylations of α,β-Unsaturated Esters. *J. Am. Chem. Soc.* **2004**, *126*, 8352-8353.
49. Moser, R.; Bošković, Ž. V.; Crowe, C. S.; Lipshutz, B. H. CuH-Catalyzed Enantioselective 1,2-Reductions of α,β-Unsaturated Ketones. *J. Am. Chem. Soc*. **2010,** *132*, 7852-7853.
50. Lipshutz, B. H.; Chrisman, W.; Noson, K.; Papa, P.; Sclafani, J. A.; Vivian, R. W.; Keith, J. M. Copper Hydride-Catalyzed Tandem 1,4-Reduction/Alkylation Reactions. *Tetrahedron*. **2000**, *56*, 2779-2788.
51. Zhao, Y.; Truhlar, D. The M06 suite of density functionals for main group thermochemistry, thermochemical kinetics, noncovalent interactions, excited states, and transition elements: two new functionals and systematic testing of four M06-class functionals and 12 other functional. *Theor. Chem. Acc*. **2008**, *120*, 215-241.
52. Zhao, Y.; Truhlar, D. Density Functionals with Broad Applicability in Chemistry. *Acc. Chem. Res*. **2008**, *41*, 157-167.
53. Bryantsev, V. S.; Diallo, M. S.; Duin, A. C. T.; Goddard III, W. A. Evaluation of B3LYP, X3LYP, and M06-Class Density Functionals for Predicting the Binding Energies of Neutral, Protonated, and Deprotonated Water Clusters. *J. Chem. Theory Comput*. **2009**, *5*, 1016-1026.
54. Jacquemin, D.; Perpète, E. A.; Ciofini, I.; Adamo, C.; Valero, R.; Zhao, Y.; Truhlar, D. G. On the Performances of the M06 Family of Density Functionals for Electronic Excitation Energies, *J. Chem. Theory Comput*. **2010**, *6*, 2071-2085
55. Shi, S. L.; Xu, L. W.; Oisaki, K.; Kanai, M.; Shibasaki, M. Identification of Modular Chiral Bisphosphines Effective for Cu(I)-Catalyzed Asymmetric Allylation and Propargylation of Ketones. *J. Am. Chem. Soc*. **2010**, *132*, 6638-6639.
56. Yang, Y.; Perry, I. B.; Lu, G.; Liu, P.; Buchwald, S. L. Copper-catalyzed asymmetric addition of olefin-derived nucleophiles to ketones. *Science*. **2016**, *353*, 144-150.
57. Liu, H. Y.; Zhang, W.; He, L.; Luo, M. L.; Qin, S. Computational investigations on the phosphine-ligated CuH-catalyzed conjugate reduction of α-β unsaturated ketones: regioselectivity and stereoselectivity. *RSC Adv*. **2014**, *4*, 5726-5733.
58. Zhang, W.; Li, W. Y.; Qin, S. Origins of enantioselectivity in the chiral diphosphine-ligated CuH-catalyzed asymmetric hydrosilylation of ketones. *Org. Biomol. Chem*. **2012**, *10*, 597-604.
59. Hong, S.; Huber, S. M.; Gagliardi, L.; Cramer, C. C.; Tolman, W. B. Copper(I)-r-Ketocarboxylate Complexes: Characterization and O2 Reactions That Yield Copper-Oxygen Intermediates Capable of Hydroxylating Arenes. *J. Am. Chem. Soc*. **2007**, *129*, 14190-14192.
60. Bar-Nahum, I.; Gupta, A. K.; Huber, S. M.; Ertem, M. Z.; Cramer, C. J.; Tolman, W. B. Reduction of Nitrous Oxide to Dinitrogen by a Mixed Valent Tricopper-Disulfido Cluster. *J. Am. Chem. Soc*. **2009**, *131*, 2812-2814.
61. Cramer, C. J.; Gour, J. R.; Kinal, A.; Wloch, M.; Piecuch, P.; Moughal Shahi, A. R.; Gagliardi, L. Stereoelectronic Effects on Molecular Geometries and State-Energy Splittings of Ligated Monocopper Dioxygen Complexes. *J. Phys. Chem. A*. **2008**, *112*, 3754-3767.
62. Tabuchi, K.; Ertem, M. Z.; Sugimoto, H.; Kunishita, A.; Tano, T.; Fujieda, N.; Cramer, C. J.; Itoh, S. Reactions of Copper(II)-Phenol Systems with O2: Models for TPQ Biosynthesis in Copper Amine Oxidases. *Inorg. Chem*. **2011**, *50*, 1633-1647.
63. Kumsapaya, C.; Bobuatong, K.; Khongpracha, P.; Tantirungrotechai, Y.; Limtrakul, J. Mechanistic Investigation on 1,5- to 2,6-Dimethylnaphthalene Isomerization Catalyzed by Acidic β Zeolite: ONIOM Study with an M06-L Functional. *J. Phys. Chem. C*. **2009**, *113*, 16128-16137.
64. Marenich, A. V.; Cramer, C. J.; Truhlar, D. G. Universal Solvation Model Based on Solute Electron Density and on a Continuum Model of the Solvent Defined by the Bulk Dielectric Constant and Atomic Surface Tensions. *J. Phys. Chem. B*. **2009**, *113*, 6378-6396.
65. Saielli, G. Differential Solvation Free Energies of Oxonium and Ammonium Ions: Insights from Quantum Chemical Calculations. *J. Phys. Chem. A*. **2010,** 114, 7261-7265.
66. Gusev, D. G. Assessing the Accuracy of M06-L Organometallic Thermochemistry. *Organometallics*. **2013**, *32*, 4239-4243.

67. Chen, X. B.; Liu, Z. C.; Lin, X. R.; Huang, R.; Yan, Sh. J.; Lin, J. Highly Diastereoselective Convergent Synthesis of Polycyclic Pyrroles with Consecutive Quaternary Stereocenters: Cascade Construction of Multiple C–C and C–Hetero Bonds. *ACS Sustainable Chem. Eng*. **2014**, *2*, 2391-2398.
68. Ribeiro, R. F.; Marenich, A. V.; Cramer, C. J.; Truhlar, D. G. Prediction of SAMPL2 aqueous solvation free energies and tautomeric ratios using the SM8, SM8AD, and SMD solvation models. *J. Comput. Aided Mater*. **2010**, *24*, 317-333.
69. Marenich, A. V.; Cramer, C. J.; Truhlar, D. G. Performance of SM6, SM8, and SMD on the SAMPL1 Test Set for the Prediction of Small-Molecule Solvation Free Energies. *J. Phys. Chem. B*. **2009**, *113*, 4538-4543.
70. Halim, M. A.; Shaw, D. M.; Poirier, R. A. Medium effect on the equilibrium geometries, vibrational frequencies and solvation energies of sulphanilamide. *THEOCHEM*. **2010**, *960*, 63-72.
71. Saielli, G. J. Differential Solvation Free Energies of Oxonium and Ammonium Ions: Insights from Quantum Chemical Calculations. *Phys. Chem. A*. **2010**, *114*, 7261-7265.
72. Kumsapaya, C.; Bobuatong, K.; Khongpracha, P.; Tantirungrotechai, Y.; J. Limtrakul, Mechanistic Investigation on 1,5- to 2,6-Dimethylnaphthalene Isomerization Catalyzed by Acidic Zeolite: ONIOM Study with an M06-L Functional. *J. Phys. Chem. C*. **2009**, *113*, 16128-16137.
73. Tran, A. T.; Liu, P.; Houk, K. N.; Nicholas, K. M. Regioselectivity in the Cu(I)-Catalyzed [4+2]-Cycloaddition of 2-Nitrosopyridine with Unsymmetrical Dienes. *J. Org. Chem*. **2014,** *79*, 5617-5626.
74. Frisch, M. J. et al. Gaussian 09 (Revision A.02), see ESI. †.